FLUCOME 2009
10th International Conference on Fluid Control, Measurements, and Visualization
August 17–21, 2009, Moscow, Russia

EFFECT OF FREE-STREAM BOUNDARY-LAYER THICKNESS ON AEROACOUSTIC CHARACTERISTICS OF OPEN CAVITY FLOW

Yang Dang-guo[1], Fan Zhao-lin[2] and Luo Xin-fu[3]

ABSTRACT

Pressure fluctuation measurement was performed inside rectangular-box cavities in an experiment conducted in a 0.6-Meter Transonic and Supersonic Wind-tunnel. The cavity length-to-depth ratio was 8 for the two experiments. The data presented herein were obtained over a Mach number of 1.5 at a Reynolds number of 2.26×10^{7} per meter with different boundary-layer thicknesses of approximately 24mm and 5.5mm. The experimental angle of attack, yawing and rolling angles were 0°. The rules were revealed governing the influence of different free-stream boundary-layer thickness on Sound pressure level (SPL) distributions and sound pressure frequency spectrum (SPFS) characteristics. The results indicate that decrease in the ratio of free-stream boundary-layer thickness to cavity depth (δ/D) causes flow oscillation amplification, peak frequency splitting and shifting phenomena of open cavity tones in the low-frequency region.

Keywords: Open cavity, Boundary-layer thickness, Aeroacoustic characteristics

INTRODUCTION

High-speed cavity flow is a common occurrence for aerospace and aeronautical vehicles. Complex unsteady flow characteristics therein are a significant concern in aerospace applications. Flow-field over cavities features boundary-layer separation, shear-layer instabilities, vortex shedding, noise radiation, shock wave/boundary-layer interactions and self-sustained flow oscillation. Flow oscillation frequencies and pressure fluctuation amplitude depend on cavity geometry and external flow properties. For cavities inside aircrafts utilized to store weapons, the maximum SPL can be 170dB [1], which damage components of aircrafts and disturb safety separation of storing weapons. The severe acoustic environment can represent a potential hazard to apparatuses' sensitivities inside cavity.

Numerous investigations on cavity flow characteristics had been conducted over the past several decades [1~15]. Pressure fluctuation distributions inside cavity had been researched by M B Tracy and E B Plentovich at subsonic and transonic speeds [4, 5]. Since the 1980s numerical method has been utilized [2, 6, 7, 9, 10, 12], which indicated that there were complex cavity flow-field characteristics. The basic cavity flow field was categorized into three types in terms of static pressure distributions inside cavity at different cavity length to depth ratio (L/D) by Stallings and M B Tracy et al, namely, open cavity flow for $L/D<10$, transitional cavity flow for $10\leqslant L/D\leqslant13$ and closed cavity flow for $L/D>13$,. Cavity flow oscillation and aeroacoustic characteristics are influenced by cavity geometrical and free-stream flow parameters.

The purpose of this study is to analyze effect of different free-stream boundary-layer thickness on aeroacoustic characteristics of open cavity flow.

1 Corresponding author: High-speed Aerodynamics Institute, China Aerodynamics Research and Development Center, e-mail: cardc@my-public.sc.cninfo.net

2 High-speed Aerodynamics Institute, China Aerodynamics Research and Development Center

3 High-speed Aerodynamics Institute, China Aerodynamics Research and Development Center

EXPERIMENTAL METHODS

FACILITIES AND INSTRUMENTATIONS

The wind tunnel is a half-circumfluence intermittent transonic and supersonic wind-tunnel with in experimental cross section of 0.6m by 0.6m High-speed aerodynamics institute of China Aerodynamics Research and Development Center. The pressure fluctuation measurements were accomplished by dynamic pressure transducers with a full-scale range of ±10 Psid and an inherent frequency of 200 KHz, and the transducers are miniature, high-sensitive and piezoresistive.

MODEL DESCRIPTION

Pressure fluctuation taps were installed along the centerline on the cavity floor. The first model was of L=80mm, W=55mm and D=10mm, which was installed on a special window in wind-tunnel side-wall. The second model was of L=267mm, W=104mm and D=33.375mm, which was within a rectangle plate installed on the special window in wind-tunnel side-wall. The photographs of the two models were shown in Fig.1 and Fig.2, respectively.

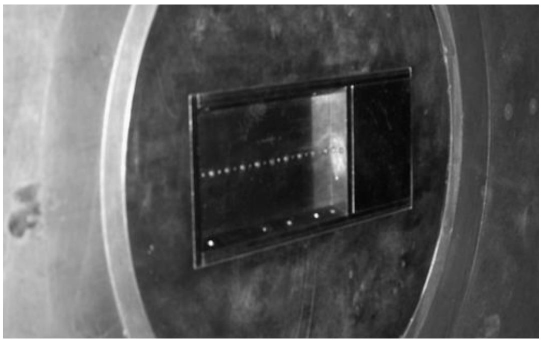

Fig.1. The first model

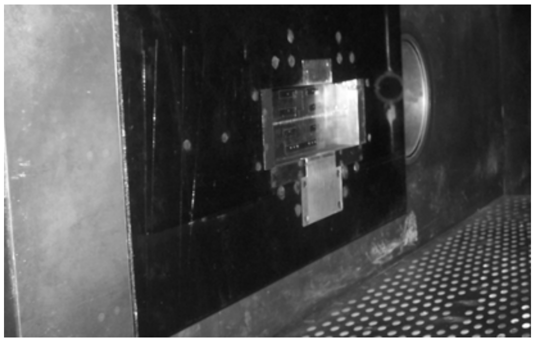

Fig.2. The second model

EXPERIMENTAL CONDITIONS

The angle of attack, yawing and rolling angles were 0° in the experiment. The length-to-depth ratio of cavities (L/D) was 8.The experimental Mach number was 1.5. The experimental Reynolds number was 2.26×10^7 per meter.

BOUNDARY-LAYER THICKNESS MEASUREMENT

For the first model, roughness webbing (3mm width) was affixed on wind-tunnel side-wall in front of the model to obtain turbulent boundary-layer over it. Total pressure distributions were measured by pressure measurement rake (shown in Fig.3). For the second model, roughness webbing was affixed on the plate upstream of the model and Peter tube (see Fig.4) was utilized to obtain total pressure distributions.

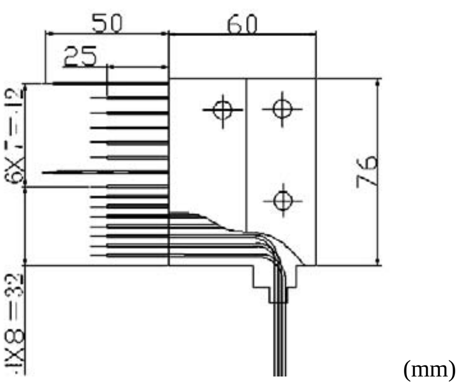

Fig.3. Pressure measurement rake

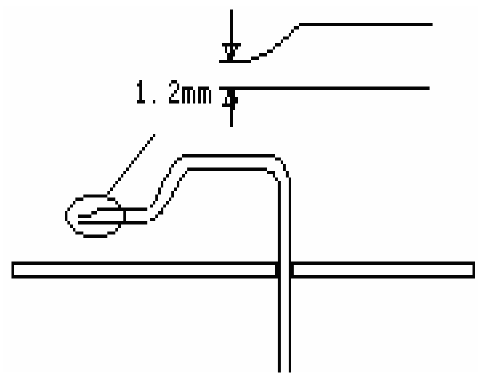

Fig.4. Peter tube

DATA PROCESSING

The highest frequency for analyzing pressures fluctuation data was 10KHz, and the frequency band distinguished was 4.88Hz. The sample length was 1024. The Hanning window and ensemble average of 64 samples were made to decrease the system difference.

Free-stream boundary-layer thickness δ was determined when non-dimensional velocity within boundary-layer was 0.99. The boundary-layer thickness (δ) and the ratio of the boundary-layer thickness to cavity depth (δ/D) for the first and the second models are shown in Table 1.

Table 1. Measurement results of the boundary-layer thickness

	δ(mm)	δ/D
The first model	24	2.4
The second model	5.5	0.16

SPL denotes pressure fluctuation magnitude, which was calculated by Eq. (1). SPFS denotes frequency characteristics of pressure fluctuation, which was calculated by Eq. (2). f denotes oscillation frequency. P_{rms} is the root-mean-square of the pressure fluctuation, which was obtained by integrating the power spectral density in the frequency band of 0～10kHz and extracting the square root. P_{ref} is the benchmark sound pressure, 20μPa, and SPFS is sound pressure spectral energy on the different discrete frequencies. $P(f)$ is the sound pressure spectral density function calculated by FFT, which was defined by Eq. (3).

$$\mathrm{SPL} = 10\lg\frac{P_{rms}^2}{P_{ref}^2} \quad (1)$$

$$\mathrm{SPFS} = 10\lg\frac{P(f)}{p_{ref}^2} \quad (2)$$

$$P(f) = \lim_{\Delta f \to 0}\frac{1}{\Delta f}\left[\lim_{T\to\infty}\frac{1}{T}\int_0^T p^2(t,f,\Delta f)\,dt\right] \quad (3)$$

DISCUSSION OF RESULTS

The effect of cavity width-to-depth ratio (W/D) on aeroacoustic characteristics of open cavity flow was little according to experimental results (Robert L. Stallings, Jr. Floyd J Wilcox and Dana K Forrest, 1991). The differences in the two experimental results are attributable to δ/D at same M and L/D. The free-stream shear-layer bridges over open cavity and has little influence on flow and acoustic radiation inside the cavity, so the SPFS characteristics of different measurement positions on the cavity floor at 0～5000Hz with L/D=8 and M=1.5 are similar, as shown in Fig.5. Experimental results at X/L=0.987 are utilized to analyze SPFS characteristics.

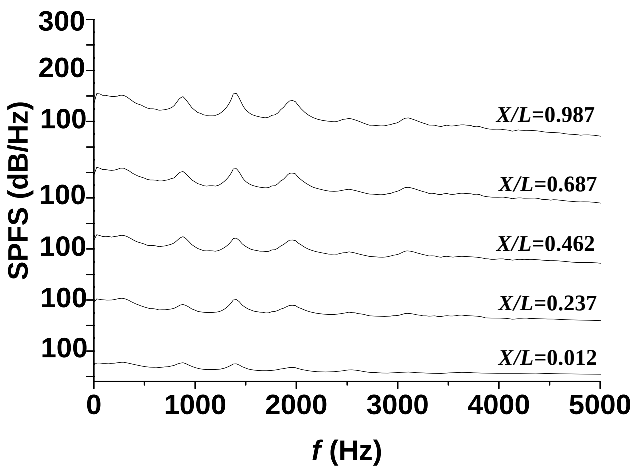

Fig.5. SPFS characteristics at different positions(*L/D*=8, *M*=1.5)

Fig.6. and Fig.7 show SPL distributions and SPFS characteristics of open cavity flow (*L/D*=8) at *M*=1.5, respectively. SPL is low in the front part inside the cavity due to free-stream shear-layer separation and expansion into the cavity. Shedding vortexes in the shear-layer bridge the middle part of the cavity and impinge the cavity rear face, which induces SPL increase there and acoustic tones at discrete frequencies. The acoustic feedback mechanism is understood to be reinforcement between instabilities in the shear-layer and sound-wave radiation from the back to the front of the cavity, and self-sustained flow oscillation is generated which results in severer cavity noise. As shown in Figure 6, for different *δ/D*, SPL distributions are similar. Decrease in *δ/D* makes pressure fluctuation severer in the shear-layer and causes interactional energy to increase between the shear-layer and flow inside the cavity, which gives rise to SPL. The decrease also shortens the cycle from impingement of the shear-layer and the rear face, acoustic generation, acoustic radiation to new impingement. The resonance frequencies shift to the low frequency region. At $0 < f < 2000$Hz, SPL increase is obvious at peak frequencies of acoustic tones. In a word, *δ/D* decrease causes amplitude magnification of acoustic tones and generates more peak oscillation frequencies in low frequency region for open cavity flow (*L/D*=8).

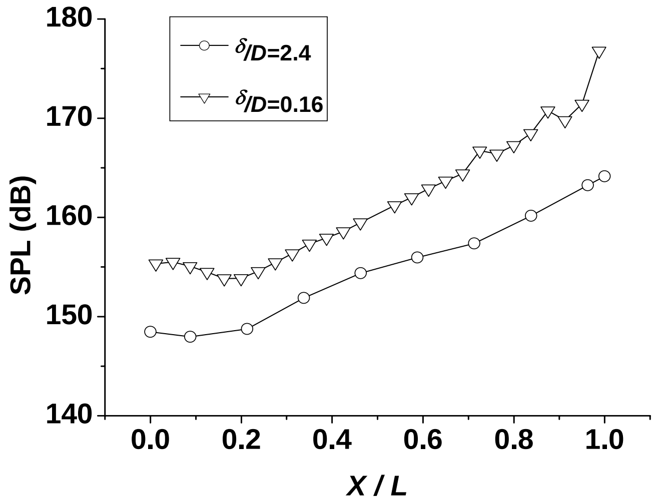

Fig.6. SPL distributions of open cavity flow

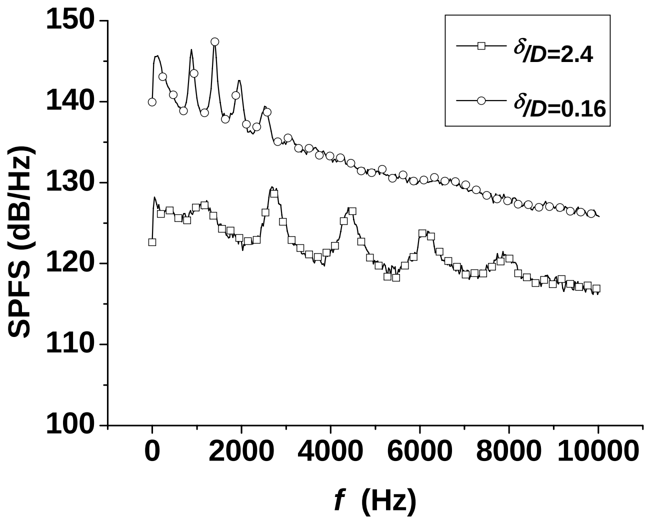

Fig.7. SPFS characteristics of open cavity flow at the position (*X/L*=0.987)

CONCLUSIONS

The intention of this paper is to extend the analysis of effect of free-stream boundary-layer thickness on cavity aeroacoustic characteristics. It indicates that δ/D influences SPL distributions, SPFS characteristics and flow oscillation peak frequencies inside the open cavity. Decrease in δ/D induces SPL increase at the same measurement position on the cavity floor. It leads to flow oscillation amplification, peak frequency splitting and shifting phenomena of acoustic tones mostly in the low-frequency region for open cavity flow.

ACKNOWLEDGEMENTS

We would like to extend our appreciation to Professor FAN Zhao-lin for his helpful comments, and for his suggestion on theoretical analysis of unsteady cavity flow characteristics. We would also like to thank High-speed Aerodynamic Institute of China Aerodynamics Research and Development Center for affording testing facilities. The researched work was supported by Government Contract.

REFERENCES

Robert L Stallings. (March-April 1983), “Store Separation from Cavity at Supersonic Flight Speeds,” Spacecraft, 20(2).

E B Plentovich. (1990), “Three-Dimensional Cavity Flow Fields at Subsonic and Transonic Speeds,” NASA-TM-4209.

Robert L. Stallings, Floyd J Wilcox, and Dana K Forrest (1991), “Measurements of Forces, Moments, and Pressures on a Generic Store Separating From a Box Cavity at Supersonic Speeds,” NASA-TP-3110.

M B Tracy and E B Plentovich (1993), “Characterization of Cavity Flow Fields Using Pressure Date Obtained in the Langley 0.3-Meter Transonic Cryogenic Tunnel,” NASA-TM-4436.

E B Plentovich, et al (1993), “Experiment Cavity Pressure Measurements at Subsonic and Transonic Speeds,” NASA Technical Paper 3358.

J C Pereira (March 1995), “Experiment and Numerical Investigation of Flow Oscillation in a Rectangular Cavity,” Transitions of ASM, Vol.117.

Robert Murray and Gregory S Elliott (1997), “The Compressible Shear-layer over a Two-Dimensional Cavity,” American of Aeronautics and Astronautics Inc.

J Henderson, K Badcock, and B E Richards (2000), “Subsonic and Transonic Transitional Cavity Flows,” AIAA Paper 2000-1966.

E Lillberg and C Fureby (2000), “Large Eddy Simulations of Supersonic Cavity Flow,” AIAA Paper 2000-2411.

CHING-WEI M S and PHILIP J M (2001), “Comparison of two-and-three-dimensional turbulent cavity flows,” AIAA Paper 2001-0511.

Lawrence S Ukeiley, Michael K Ponton, John M Seiner, and Bernard Jansen (2002), “Suppression of Pressure Loads in Cavity Flow,” AIAA Paper 2002-0661.

A Hamed, D Basu, and K Das (2003), “Detached Eddy Simulations of Supersonic Flow Over Cavity,” AIAA Paper 2003-549.

M Debiasi, P Yan, and J Little (2004), “An Experiment Study of Subsonic Cavity Flow-Physical Understanding and Control,” AIAA Paper 2004-2123.

N Zhang and Farrukh Alvi (2005), “Control of Cavity Tones in Supersonic Flow,” AIAA Paper 2005-0793.

P Yan, M Debiasi, and X Yuan, et al (May 2006), “Experiment Study of Linear Closed-Loop Control of Subsonic Cavity Flow,” AIAA Paper Vol.44, No.5.

APPENDIX I. NOTATION

The following symbols were used,

D	Cavity depth	[m]
f	Oscillation frequency	[Hz]
$G(f)$	Power spectrum energy	

L	Cavity length	[m]
L/D	Ratio of cavity length to depth	
M	Free-stream Mach number	
P_{ref}	Benchmark sound pressure	[Pa]
P_{rms}	Root-mean-square of the pressure fluctuation	[Pa]
$P_{rms}(f)$	Power spectrum density function	
Re	Reynolds number	
W	Cavity width	[m]
X/L	Ratio of measurement position to cavity length	
δ	Boundary-layer thickness	[m]
δ/D	Ratio of boundary-layer thickness to cavity depth	
SPL	Sound pressure level	[dB]
SPFS	Sound pressure frequency spectrum	[dB/Hz]